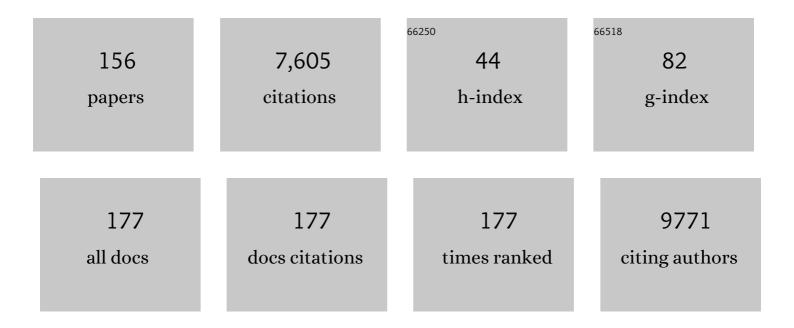
Olaf Dietrich

List of Publications by Year in descending order

Source: https://exaly.com/author-pdf/565949/publications.pdf Version: 2024-02-01



#	Article	IF	CITATIONS
1	Individually unique dynamics of cortical connectivity reflect the ongoing intensity of chronic pain. Pain, 2022, 163, 1987-1998.	2.0	10
2	Evaluation of an anthropomorphic ion chamber and 3D gel dosimetry head phantom at a 0.35 T MR-linac using separate 1.5 T MR-scanners for gel readout. Zeitschrift Fur Medizinische Physik, 2022, , .	0.6	3
3	Tuning the Synergistic Interplay between Clinical MRI Contrast Agents and MR-Active Metal–Organic Framework Nanoparticles. Chemistry of Materials, 2022, 34, 3862-3871.	3.2	6
4	End-to-End Deep Learning Approach for Perfusion Data: A Proof-of-Concept Study to Classify Core Volume in Stroke CT. Diagnostics, 2022, 12, 1142.	1.3	2
5	Multi-shell Diffusion MRI Models for White Matter Characterization in Cerebral Small Vessel Disease. Neurology, 2021, 96, e698-e708.	1.5	33
6	Integration of spatial distortion effects in a 4D computational phantom for simulation studies in extraâ€cranial MRIâ€guided radiation therapy: Initial results. Medical Physics, 2021, 48, 1646-1660.	1.6	1
7	Animal tissue-based quantitative comparison of dual-energy CT to SPR conversion methods using high-resolution gel dosimetry. Physics in Medicine and Biology, 2021, 66, 075009.	1.6	13
8	Measurementâ€based range evaluation for quality assurance of CBCTâ€based dose calculations in adaptive proton therapy. Medical Physics, 2021, 48, 4148-4159.	1.6	8
9	Detecting COVID-19–related Chronic Pulmonary Injury with ¹²⁹ Xe MRI. Radiology, 2021, 301, E373-E374.	3.6	0
10	Artifact reduction of coaxial needles in magnetic resonance imaging-guided abdominal interventions at 1.5 T: a phantom study. Scientific Reports, 2021, 11, 22963.	1.6	2
11	Altered relaxation times in MRI indicate bronchopulmonary dysplasia. Thorax, 2020, 75, 184-187.	2.7	22
12	Performing Diffusion Tensor and Functional MRI in Patients with Metallic Braces. Radiology, 2020, 294, 158-159.	3.6	0
13	Clinically Approved MRI Contrast Agents as Imaging Labels for a Porous Ironâ€Based MOF Nanocarrier: A Systematic Investigation in a Clinical MRI Setting. Advanced Therapeutics, 2020, 3, 1900126.	1.6	19
14	Variable functional connectivity architecture of the preterm human brain: Impact of developmental cortical expansion and maturation. Proceedings of the National Academy of Sciences of the United States of America, 2020, 117, 1201-1206.	3.3	49
15	Analyzing the co-localization of substantia nigra hyper-echogenicities and iron accumulation in Parkinson's disease: A multi-modal atlas study with transcranial ultrasound and MRI. NeuroImage: Clinical, 2020, 26, 102185.	1.4	18
16	Early risk stratification in preterm infants with Bronchopulmonary Dysplasia via pulmonary arterial flow measurements in MRI. , 2020, , .		3
17	Improving the modelling of susceptibility-induced spatial distortions in MRI-guided extra-cranial radiotherapy. Physics in Medicine and Biology, 2019, 64, 205006.	1.6	3
18	Bayesian pharmacokinetic modeling of dynamic contrast-enhanced magnetic resonance imaging: validation and application. Physics in Medicine and Biology, 2019, 64, 18NT02.	1.6	6

#	Article	IF	CITATIONS
19	PO-1004 Simulation of tissue dependent magnetic field susceptibility effects in MRI guided radiotherapy. Radiotherapy and Oncology, 2019, 133, S554-S555.	0.3	1
20	Assessment of intravoxel incoherent motion MRI with an artificial capillary network: analysis of biexponential and phaseâ€distribution models. Magnetic Resonance in Medicine, 2019, 82, 1373-1384.	1.9	12
21	Nonuniform Fourierâ€decomposition MRI for ventilation―and perfusionâ€weighted imaging of the lung. Magnetic Resonance in Medicine, 2019, 82, 1312-1321.	1.9	23
22	Gel dosimetry for three dimensional proton range measurements in anthropomorphic geometries. Zeitschrift Fur Medizinische Physik, 2019, 29, 162-172.	0.6	22
23	Improved detection of a tumorous involvement of the mesorectal fascia and locoregional lymph nodes in locally advanced rectal cancer using DCE-MRI. International Journal of Colorectal Disease, 2018, 33, 901-909.	1.0	16
24	Diffusion imaging of the vertebral bone marrow. NMR in Biomedicine, 2017, 30, e3333.	1.6	63
25	Technical Note: Quantitative dynamic contrast-enhanced MRI of a 3-dimensional artificial capillary network. Medical Physics, 2017, 44, 1462-1469.	1.6	2
26	Hough-CNN: Deep learning for segmentation of deep brain regions in MRI and ultrasound. Computer Vision and Image Understanding, 2017, 164, 92-102.	3.0	282
27	Transient Bone Marrow Edema Syndrome versus Osteonecrosis: Perfusion Patterns at Dynamic Contrast-enhanced MR Imaging with High Temporal Resolution Can Allow Differentiation. Radiology, 2017, 283, 478-485.	3.6	36
28	MR imaging differentiation of Fe2+ and Fe3+ based on relaxation and magnetic susceptibility properties. Neuroradiology, 2017, 59, 403-409.	1.1	36
29	Improving material separation of high-flux whole-body photon counting computed tomography by K-edge pre-filtration. , 2017, , .		0
30	T1 relaxation time constants, influence of oxygen, and the oxygen transfer function of the human lung at 1.5 T—A meta-analysis. European Journal of Radiology, 2017, 86, 252-260.	1.2	9
31	PO-0809: A 3D polymer gel dosimeter coupled to a patient-specific anthropomorphic phantom for proton therapy. Radiotherapy and Oncology, 2017, 123, S432-S433.	0.3	0
32	Detection of single-phase CTA occult vessel occlusions in acute ischemic stroke using CT perfusion-based wavelet-transformed angiography. European Radiology, 2017, 27, 2657-2664.	2.3	19
33	Intravoxel Incoherent Motion Magnetic Resonance Imaging in Partially Nephrectomized Kidneys. Investigative Radiology, 2016, 51, 323-330.	3.5	18
34	Detection of pulmonary embolism with free-breathing dynamic contrast-enhanced MRI. Journal of Magnetic Resonance Imaging, 2016, 43, 887-893.	1.9	11
35	Classification of arterial and venous cerebral vasculature based on wavelet postprocessing of CT perfusion data. Medical Physics, 2016, 43, 702-709.	1.6	1
36	Proton MRI Based Ventilation Imaging: Oxygen-Enhanced Lung MRI and Alternative Approaches. Medical Radiology, 2016, , 137-162.	0.0	1

#	Article	IF	CITATIONS
37	Improving material decomposition by spectral optimization of photon counting computed tomography. Proceedings of SPIE, 2016, , .	0.8	2
38	Surrogate MRI markers for hyperthermia-induced release of doxorubicin from thermosensitive liposomes in tumors. Journal of Controlled Release, 2016, 237, 138-146.	4.8	40
39	Comparison of contrast-enhanced modified T1-weighted 3D TSE black-blood and 3D MP-RAGE sequences for the detection of cerebral metastases and brain tumours. European Radiology, 2016, 26, 1818-1825.	2.3	31
40	LSC Abstract – Early biomarkers indicating the development of neonatal chronic lung disease defined by clinical and imaging parameters. , 2016, , .		0
41	Material Characterization of Dual-Energy Computed Tomographic Data Using Polar Coordinates. Journal of Computer Assisted Tomography, 2015, 39, 134-139.	0.5	1
42	Flip angle-optimized fast dynamic T ₁ mapping with a 3D gradient echo sequence. Magnetic Resonance in Medicine, 2015, 73, 1158-1163.	1.9	5
43	Physiological Background of Differences in Quantitative Diffusion-Weighted Magnetic Resonance Imaging Between Acute Malignant and Benign Vertebral Body Fractures. Journal of Computer Assisted Tomography, 2015, 39, 643-648.	0.5	5
44	Wavelet-based calculation of cerebral angiographic data from time-resolved CT perfusion acquisitions. European Radiology, 2015, 25, 2354-2361.	2.3	11
45	Validation of a method to differentiate arterial and venous vessels in CT perfusion data using linear combinations of quantitative time-density curve characteristics. European Radiology, 2015, 25, 2937-2944.	2.3	7
46	Feasibility of spectral CT imaging for the detection of liver lesions with gold-based contrast agents – A simulation study. Physica Medica, 2015, 31, 875-881.	0.4	22
47	MR volumetric assessment of endolymphatic hydrops. European Radiology, 2015, 25, 585-595.	2.3	86
48	Hepatic steatosis: Effect on hepatocyte enhancement with gadoxetate disodiumâ€enhanced liver MR imaging. Journal of Magnetic Resonance Imaging, 2014, 39, 42-50.	1.9	13
49	Diffusion-weighted MRI of the Prostate: Advantages of Zoomed EPI with Parallel-transmit-accelerated 2D-selective Excitation Imaging. European Radiology, 2014, 24, 3233-3241.	2.3	78
50	Assessment of Pulmonary Perfusion With Breath-Hold and Free-Breathing Dynamic Contrast-Enhanced Magnetic Resonance Imaging. Investigative Radiology, 2014, 49, 382-389.	3.5	26
51	Imaging cell size and permeability in biological tissue using the diffusion-time dependence of the apparent diffusion coefficient. Physics in Medicine and Biology, 2014, 59, 3081-3096.	1.6	9
52	JOURNAL CLUB: Quantitative Evaluation of Benign and Malignant Vertebral Fractures With Diffusion-Weighted MRI: What Is the Optimum Combination of b Values for ADC-Based Lesion Differentiation With the Single-Shot Turbo Spin-Echo Sequence?. American Journal of Roentgenology, 2014, 203, 582-588.	1.0	32
53	Parallel-transmit-accelerated spatially-selective excitation mri for reduced-fov diffusion-weighted-imaging of the pancreas. European Journal of Radiology, 2014, 83, 1709-1714.	1.2	31
54	Feasibility study of spectral computed tomography (CT) with gold as a new contrast agent. Proceedings of SPIE, 2014, , .	0.8	0

#	Article	IF	CITATIONS
55	Development and evaluation of a novel designed breast CT system. , 2014, , .		0
56	Monitoring Early Response to Anti-Angiogenic Therapy: Diffusion-Weighted Magnetic Resonance Imaging and Volume Measurements in Colon Carcinoma Xenografts. PLoS ONE, 2014, 9, e106970.	1.1	8
57	Techniques for Diffusion and Perfusion Assessment in Bone-Marrow MRI. Medical Radiology, 2013, , 339-354.	0.0	1
58	Quantification of Pulmonary Perfusion with Free-Breathing Dynamic Contrast-Enhanced MRI – A Pilot Study in Healthy Volunteers. RoFo Fortschritte Auf Dem Gebiet Der Rontgenstrahlen Und Der Bildgebenden Verfahren, 2013, 185, e2-e2.	0.7	1
59	Quantification of Pulmonary Perfusion with Free-Breathing Dynamic Contrast-Enhanced MRI – A Pilot Study in Healthy Volunteers. RoFo Fortschritte Auf Dem Gebiet Der Rontgenstrahlen Und Der Bildgebenden Verfahren, 2013, 185, 1175-1181.	0.7	7
60	Diffusion-Tensor Imaging of Human Articular Cartilage Specimens with Early Signs of Cartilage Damage. Radiology, 2013, 266, 831-841.	3.6	72
61	Free Breathing Real-Time Cardiac Cine Imaging With Improved Spatial Resolution at 3 T. Investigative Radiology, 2013, 48, 158-166.	3.5	10
62	In vivo monitoring of sorafenib therapy effects on experimental prostate carcinomas using dynamic contrast-enhanced MRI and macromolecular contrast media. Cancer Imaging, 2013, 13, 557-566.	1.2	7
63	Articular Cartilage: In Vivo Diffusion-Tensor Imaging. Radiology, 2012, 262, 550-559.	3.6	103
64	Comparison of Qualitative and Quantitative Evaluation of Diffusion-Weighted MRI and Chemical-Shift Imaging in the Differentiation of Benign and Malignant Vertebral Body Fractures. American Journal of Roentgenology, 2012, 199, 1083-1092.	1.0	60
65	Perfusion MRI for Monitoring the Effect of Sorafenib on Experimental Prostate Carcinoma: A Validation Study. American Journal of Roentgenology, 2012, 198, 384-391.	1.0	22
66	Dynamic Contrast-Enhanced Computed Tomography Imaging Biomarkers Correlated With Immunohistochemistry for Monitoring the Effects of Sorafenib on Experimental Prostate Carcinomas. Investigative Radiology, 2012, 47, 49-57.	3.5	38
67	Value of oxygenâ€enhanced MRI of the lungs in patients with pulmonary hypertension: A qualitative and quantitative approach. Journal of Magnetic Resonance Imaging, 2012, 35, 86-94.	1.9	8
68	Erratum to "Combined diffusion-weighted and dynamic contrast-enhanced imaging of patients with acute osteoporotic vertebral fractures―[Eur. J. Radiol. 76 (2010) 298–303]. European Journal of Radiology, 2011, 77, 528.	1.2	0
69	Gadofosveset. Investigative Radiology, 2011, 46, 678-685.	3.5	13
70	Quantitative Analysis of the Diffusion-Weighted Steady-State Free Precession Signal in Vertebral Bone Marrow Lesions. Investigative Radiology, 2011, 46, 601-609.	3.5	27
71	Change of Diffusion Tensor Imaging Parameters in Articular Cartilage With Progressive Proteoglycan Extraction. Investigative Radiology, 2011, 46, 401-409.	3.5	41
72	Ultra-high field diffusion tensor imaging of articular cartilage correlated with histology and scanning electron microscopy. Magnetic Resonance Materials in Physics, Biology, and Medicine, 2011, 24, 247-258.	1.1	35

#	Article	IF	CITATIONS
73	Quantitative analysis of vertebral bone marrow perfusion using dynamic contrastâ€enhanced MRI: Initial results in osteoporotic patients with acute vertebral fracture. Journal of Magnetic Resonance Imaging, 2011, 33, 676-683.	1.9	32
74	Oxygen-Enhanced MRI of the Lungs: Intraindividual Comparison Between 1.5 and 3 Tesla. RoFo Fortschritte Auf Dem Gebiet Der Rontgenstrahlen Und Der Bildgebenden Verfahren, 2011, 183, 358-364.	0.7	9
75	Test–retest reproducibility of the defaultâ€mode network in healthy individuals. Human Brain Mapping, 2010, 31, 237-246.	1.9	174
76	<i>T</i> ₂ measurement in articular cartilage: Impact of the fitting method on accuracy and precision at low SNR. Magnetic Resonance in Medicine, 2010, 63, 181-193.	1.9	137
77	Quantitative Pulmonary Perfusion Magnetic Resonance Imaging. Investigative Radiology, 2010, 45, 7-14.	3.5	35
78	Analysis of Signal Dynamics in Oxygen-Enhanced Magnetic Resonance Imaging. Investigative Radiology, 2010, 45, 165-173.	3.5	12
79	Diffusion Tensor Imaging (DTI) of the Kidney at 3 Tesla–Feasibility, Protocol Evaluation and Comparison to 1.5 Tesla. Investigative Radiology, 2010, 45, 245-254.	3.5	94
80	Multiparameter MRI assessment of normal-appearing and diseased vertebral bone marrow. European Radiology, 2010, 20, 2679-2689.	2.3	30
81	Measurement of perfusion and permeability from dynamic contrastâ€enhanced MRI in normal and pathological vertebral bone marrow. Magnetic Resonance in Medicine, 2010, 64, 115-124.	1.9	24
82	High-resolution black-blood contrast-enhanced <i>T</i> ₁ weighted images for the diagnosis and follow-up of intracranial arteritis. British Journal of Radiology, 2010, 83, e182-e184.	1.0	55
83	Correction to: British Journal of Radiology (2010) 83, e182-e184 doi: 10.1259/bjr/74101656. British Journal of Radiology, 2010, 83, 1090-1090.	1.0	Ο
84	Technical aspects of MR diffusion imaging of the body. European Journal of Radiology, 2010, 76, 314-322.	1.2	121
85	Diffusion and perfusion imaging of bone marrow. European Journal of Radiology, 2010, 76, 323-328.	1.2	89
86	Combined diffusion-weighted and dynamic contrast-enhanced imaging of patients with acute osteoporotic vertebral fractures. European Journal of Radiology, 2010, 76, 298-303.	1.2	43
87	Diffusion-Weighted Imaging of Bone Marrow. Seminars in Musculoskeletal Radiology, 2009, 13, 134-144.	0.4	87
88	Regional networks underlying interhemispheric connectivity: An EEG and DTI study in healthy ageing and amnestic mild cognitive impairment. Human Brain Mapping, 2009, 30, 2098-2119.	1.9	85
89	Halfâ€fourierâ€acquisition singleâ€shot turbo spinâ€echo (HASTE) MRI of the lung at 3 Tesla using parallel imaging with 32â€receiver channel technology. Journal of Magnetic Resonance Imaging, 2009, 30, 541-546.	1.9	21
90	Voxel-based reproducibility of T2 relaxation time in patellar cartilage at 1.5 T with a new validated 3D rigid registration algorithm. Magnetic Resonance Materials in Physics, Biology, and Medicine, 2009, 22, 229-239.	1.1	15

#	Article	IF	CITATIONS
91	High resolution carotid black-blood 3T MR with parallel imaging and dedicated 4-channel surface coils. Journal of Cardiovascular Magnetic Resonance, 2009, 11, 41.	1.6	51
92	MRI of respiratory dynamics with 2D steady-state free-precession and 2D gradient echo sequences at 1.5 and 3 Tesla: an observer preference study. European Radiology, 2009, 19, 391-399.	2.3	22
93	Magnetic resonance imaging of the cervical spine: comparison of 2D T2-weighted turbo spin echo, 2D T2*weighted gradient-recalled echo and 3D T2-weighted variable flip-angle turbo spin echo sequences. European Radiology, 2009, 19, 713-721.	2.3	58
94	Thoracic and abdominal MRA with gadofosveset: Influence of injection rate on vessel signal and image quality. European Radiology, 2009, 19, 1932-1938.	2.3	15
95	Time-Resolved 3D Pulmonary Perfusion MRI. Investigative Radiology, 2009, 44, 525-531.	3.5	28
96	MRI of Pulmonary Ventilation. Medical Radiology, 2009, , 35-90.	0.0	0
97	Renal T2â€weighted turboâ€spinâ€echo imaging with BLADE at 3.0 Tesla: Initial experience. Journal of Magnetic Resonance Imaging, 2008, 27, 148-153.	1.9	34
98	Magnetic resonance noise measurements and signalâ€quantization effects at very low noise levels. Magnetic Resonance in Medicine, 2008, 60, 1477-1487.	1.9	15
99	Influence of multichannel combination, parallel imaging and other reconstruction techniques on MRI noise characteristics. Magnetic Resonance Imaging, 2008, 26, 754-762.	1.0	199
100	Basics of Magnetic Resonance Imaging and Magnetic Resonance Spectroscopy. , 2008, , 3-167.		12
101	Artifacts in 3-T MRI: Physical background and reduction strategies. European Journal of Radiology, 2008, 65, 29-35.	1.2	216
102	Black-Blood Diffusion-Weighted EPI Acquisition of the Liver with Parallel Imaging. Investigative Radiology, 2008, 43, 261-266.	3.5	101
103	Diffusion Tensor Imaging of the Kidney With Parallel Imaging: Initial Clinical Experience. Investigative Radiology, 2008, 43, 677-685.	3.5	112
104	Feasibility of Gadofosveset-Enhanced Steady-State Magnetic Resonance Angiography of the Peripheral Vessels at 3 Tesla With Dixon Fat Saturation. Investigative Radiology, 2008, 43, 635-641.	3.5	36
105	Technical Prerequisites. Medical Radiology, 2008, , 77-126.	0.0	Ο
106	Fiber Connections between the Cerebral Cortex and the Corpus Callosum in Alzheimer's Disease: A Diffusion Tensor Imaging and Voxel-Based Morphometry Study. Cerebral Cortex, 2007, 17, 2276-2282.	1.6	74
107	White Matter Damage in Alzheimer Disease and Mild Cognitive Impairment: Assessment with Diffusion-Tensor MR Imaging and Parallel Imaging Techniques. Radiology, 2007, 243, 483-492.	3.6	197
108	Intraindividual Comparison of High-Spatial-Resolution Abdominal MR Angiography at 1.5 T and 3.0 T: Initial Experience. Radiology, 2007, 244, 907-913.	3.6	49

#	Article	IF	CITATIONS
109	Lung MRI at 1.5 and 3 Tesla. Investigative Radiology, 2007, 42, 377-383.	3.5	68
110	Myocardial Perfusion Imaging With Gadobutrol: A Comparison Between 3 and 1.5 Tesla With an Identical Sequence Design. Investigative Radiology, 2007, 42, 499-506.	3.5	21
111	Myocardial First Pass Perfusion Imaging With Gadobutrol. Investigative Radiology, 2007, 42, 522-528.	3.5	15
112	Multivariate network analysis of fiber tract integrity in Alzheimer's disease. NeuroImage, 2007, 34, 985-995.	2.1	162
113	Evidence of Subcortical and Cortical Aging of the Acoustic Pathway: A Diffusion Tensor Imaging (DTI) Study. Academic Radiology, 2007, 14, 692-700.	1.3	30
114	Measurement of signalâ€ŧoâ€noise ratios in MR images: Influence of multichannel coils, parallel imaging, and reconstruction filters. Journal of Magnetic Resonance Imaging, 2007, 26, 375-385.	1.9	809
115	Dual breath-hold magnetic resonance cine evaluation of global and regional cardiac function. European Radiology, 2007, 17, 73-80.	2.3	48
116	Quantitative and qualitative characterization of vascularization and hemodynamics in head and neck tumors with a 3D magnetic resonance time-resolved echo-shared angiographic technique (TREAT)—initial results. European Radiology, 2007, 17, 1101-1110.	2.3	16
117	MR imaging of the cervical spine: assessment of image quality with parallel imaging compared to non-accelerated MR measurements. European Radiology, 2007, 17, 1147-1155.	2.3	29
118	Feasibility of a RARE-based sequence for quantitative diffusion-weighted MRI of the spine. European Radiology, 2007, 17, 2872-2879.	2.3	21
119	Myocardial tagging with steady state free precession techniques and semi-automatic postprocessing—impact on diagnostic value. European Radiology, 2007, 17, 2218-2224.	2.3	5
120	Functional renal MR imaging: an overview. Abdominal Imaging, 2007, 32, 758-771.	2.0	36
121	MRI from k-Space to Parallel Imaging. , 2007, , 3-17.		3
122	Single-Shot Pulse Sequences. , 2007, , 119-126.		5
123	Oxygen-Enhanced Imaging of the Lung. , 2007, , 429-440.		2
124	Design of Parallel-Imaging Protocols. , 2007, , 169-172.		0
125	Multicenter assessment of reliability of cranial MRI. Neurobiology of Aging, 2006, 27, 1051-1059.	1.5	96
126	Cardiac Steady-State Free Precession CINE Magnetic Resonance Imaging at 3.0 Tesla. Investigative Radiology, 2006, 41, 141-147.	3.5	42

#	Article	IF	CITATIONS
127	MRA of abdominal vessels: technical advances. European Radiology, 2006, 16, 1637-1650.	2.3	19
128	Cardiac CINE MR imaging with a 32-channel cardiac coil and parallel imaging: Impact of acceleration factors on image quality and volumetric accuracy. Journal of Magnetic Resonance Imaging, 2006, 23, 222-227.	1.9	71
129	High-resolution renal MRA: Comparison of image quality and vessel depiction with different parallel imaging acceleration factors. Journal of Magnetic Resonance Imaging, 2006, 24, 95-100.	1.9	43
130	Methods and applications of diffusion imaging of vertebral bone marrow. Journal of Magnetic Resonance Imaging, 2006, 24, 1207-1220.	1.9	66
131	High-Spatial-Resolution Multistation MR Angiography with Parallel Imaging and Blood Pool Contrast Agent: Initial Experience. Radiology, 2006, 241, 861-872.	3.6	103
132	Pulmonary Abnormalities in Immunocompromised Patients: Comparative Detection with Parallel Acquisition MR Imaging and Thin-Section Helical CT. Radiology, 2006, 241, 880-891.	3.6	106
133	A comparative evaluation of a RARE-based single-shot pulse sequence for diffusion-weighted MRI of musculoskeletal soft-tissue tumors. European Radiology, 2005, 15, 772-783.	2.3	34
134	High-resolution diffusion tensor imaging of human patellar cartilage: Feasibility and preliminary findings. Magnetic Resonance in Medicine, 2005, 53, 993-998.	1.9	141
135	Fast oxygen-enhanced multislice imaging of the lung using parallel acquisition techniques. Magnetic Resonance in Medicine, 2005, 53, 1317-1325.	1.9	35
136	Practical approaches to the evaluation of signal-to-noise ratio performance with parallel imaging: Application with cardiac imaging and a 32-channel cardiac coil. Magnetic Resonance in Medicine, 2005, 54, 748-754.	1.9	274
137	High-Spatial-Resolution MR Angiography of Renal Arteries with Integrated Parallel Acquisitions: Comparison with Digital Subtraction Angiography and US. Radiology, 2005, 235, 687-698.	3.6	115
138	Pulmonary Arterial Hypertension: Diagnosis with Fast Perfusion MR Imaging and High-Spatial-Resolution MR Angiography—Preliminary Experience. Radiology, 2005, 236, 694-703.	3.6	125
139	Measurement of basal forebrain atrophy in Alzheimer's disease using MRI. Brain, 2005, 128, 2626-2644.	3.7	213
140	Cardiovascular Screening with Parallel Imaging Techniques and a Whole-Body MR Imager. Radiology, 2005, 236, 300-310.	3.6	84
141	Techniques for diffusion-weighted imaging of bone marrow. European Journal of Radiology, 2005, 55, 64-73.	1.2	41
142	High-resolution MR-imaging of the liver with T2-weighted sequences using integrated parallel imaging: Comparison of prospective motion correction and respiratory triggering. Journal of Magnetic Resonance Imaging, 2004, 20, 443-450.	1.9	99
143	P3-069 Reliability of multicenter MRI. Results of a phantom test and in vivo MRI measurement. Neurobiology of Aging, 2004, 25, S372.	1.5	0
144	P2-229 Fiber tract integrity in Alzheimer's disease: a voxel-based analysis of regional changes in fractional anisotropy. Neurobiology of Aging, 2004, 25, S297.	1.5	0

#	Article	IF	CITATIONS
145	Quantification of Pulmonary Blood Flow and Volume in Healthy Volunteers by Dynamic Contrast-Enhanced Magnetic Resonance Imaging Using a Parallel Imaging Technique. Investigative Radiology, 2004, 39, 537-545.	3.5	98
146	Diffusion-weighted imaging of bone marrow: current status. European Radiology, 2003, 13, 1699-1708.	2.3	110
147	Single breath-hold real-time cine MR imaging: improved temporal resolution using generalized autocalibrating partially parallel acquisition (GRAPPA) algorithm. European Radiology, 2003, 13, 1931-1936.	2.3	92
148	Renal MR angiography: Current debates and developments in imaging of renal artery stenosis. Seminars in Ultrasound, CT and MRI, 2003, 24, 255-267.	0.7	29
149	Diagnosis of renal artery stenosis with magnetic resonance angiography: update 2003. Nephrology Dialysis Transplantation, 2003, 18, 1252-1256.	0.4	36
150	Diffusion-weighted imaging of the spinal column. Neuroimaging Clinics of North America, 2002, 12, 147-160.	0.5	36
151	Diffusion-weighted imaging of the brain: comparison of stimulated- and spin-echo echo-planar sequences. Neuroradiology, 2001, 43, 442-447.	1.1	11
152	Diffusion-weighted imaging of the spine using radialk-space trajectories. Magnetic Resonance Materials in Physics, Biology, and Medicine, 2001, 12, 23-31.	1.1	34
153	Diffusion-weighted imaging of the spine using radial k-space trajectories. Magnetic Resonance Materials in Physics, Biology, and Medicine, 2001, 12, 23-31.	1.1	23
154	Noise correction for the exact determination of apparent diffusion coefficients at low SNR. Magnetic Resonance in Medicine, 2001, 45, 448-453.	1.9	130
155	Reducing motion artefacts in diffusion-weighted MRI of the brain: efficacy of navigator echo correction and pulse triggering. Neuroradiology, 2000, 42, 85-91.	1.1	35

Diffusion-weighted MRI of the bone marrow and the spine. , 0, , 144-161.

0